THE ASTROPHYSICAL JOURNAL, 549:578–589, 2001 March 1

THE STAR FORMATION HISTORY OF TRUMPLER 14 AND TRUMPLER 16

K. DEGIOIA-EASTWOOD,[1] H. THROOP,[2] AND G. WALKER[3]
Department of Physics and Astronomy, Northern Arizona University, Flagstaff, AZ 86011-6010; Kathy.Eastwood@nau.edu
AND
K. M. CUDWORTH
Yerkes Observatory, The University of Chicago, Williams Bay, Wisconsin 53191; kmc@hale.yerkes.uchicago.edu
Received 2000 April 7; accepted 2000 September 1

ABSTRACT

H-R diagrams are presented for the very young galactic clusters Trumpler 14 and Trumpler 16, which are the two most populous clusters in the region of vigorous star formation surrounding η Carinae. Point spread function photometry of UBV CCD images is presented down to $V \approx 19$ for over 560 stars in Tr 16 and 290 stars in Tr 14. We have also obtained similar data for a local background field. After determining cluster membership through proper motions from a previous work, we find that the reddening of cluster members is significantly lower than that of the local background stars. Thus, we are able to use individual reddenings to identify likely members at far deeper levels than possible with proper motions. This work has revealed a significant population of pre–main-sequence (PMS) stars in both clusters. The location of the PMS stars in the H-R diagram indicates that the theoretical "stellar birthline" of Palla & Stahler follows the locus of stars far better than that of Beech & Mitalas. Comparison with both pre– and post–main-sequence isochrones also reveals that although intermediate-mass stars have been forming continuously over the last 10 Myr, the high-mass stars formed within the last 3 Myr. There is no evidence that the formation of the intermediate-mass stars was truncated by the formation of the high-mass stars.

Subject headings: stars: formation — stars: pre–main-sequence
On-line material: machine-readable tables

1. INTRODUCTION

The star clusters Trumpler 14 and 16 are the two most populous clusters in the Great Carina Nebula, NGC 3372. Tr 16 is the parent cluster of η Carinae, now recognized as the prototypical luminous blue variable. These well-studied clusters are probably the closest approximation to 30 Doradus that have been found in our Galaxy, and provided the impetus for extending the MK spectral sequence as early as O3 (Walborn 1971). There is ongoing star formation in the molecular cloud complex associated with the region (Megeath et al. 1996). Over the years there have been extensive discussions about the possibility of anomalous extinction in the region, and whether or not the two clusters are at the same distance. The IMF of the two clusters is similar to those of other populous Milky Way clusters (Massey & Johnson 1993).

In an earlier paper (Cudworth, Martin, & DeGioia-Eastwood 1993) we presented proper motions for 600 stars belonging to these clusters (and Cr 232) with a limiting magnitude of $V \approx 15.5$. This work presents new CCD UBV photometry for over 850 stars in the two clusters, with a limiting magnitude of $V \approx 19$. The proper motions allow us to determine that the reddening for cluster members is significantly lower than that of nonmembers. The distribution of $E(B-V)$ is double-peaked, with the peak at lower values of $E(B-V)$ corresponding to members, and the peak at higher values corresponding to nonmembers. Photometry was also obtained for the stars in a local background field, and the reddening distribution for the background field is similar to the known nonmembers in the cluster fields. This reddening analysis allows us to further separate members from nonmembers (i.e., more deeply than with the proper motions) by assuming that all stars with $E(B-V)$ greater than the minimum between the two peaks are nonmembers.

The removal of probable nonmembers from the H-R diagrams allows us to address several questions about the star formation process in Tr 14 and 16. The first is whether there is evidence for the theoretical birthline, and if so, which model best agrees with the observations. We also examine the star formation history of this cluster, e.g., whether all the stars are coeval.

2. OBSERVATIONS

2.1. *Photometry*

The observations consisted of direct exposures with the 800 × 800 TI 3 CCD at CTIO, binned to 2 × 2, on the 0.91 m telescope. The filters were U, B, V, R, and Hα, although only the U, B, and V data are presented here. The scale was $0\farcs494$ pixel^{-1}, and the field of view was thus about 3.3 arcmin square. The observations of Tr 16 and the background fields were taken 1990 February 9–12 UT, and those of Tr 14 on 1990 February 14.

As shown in Figure 1, exposures were made of 14 different fields: nine covering the Tr 16 area, three covering the Tr 14 area, and two representing a local background field. The fields were overlapped slightly to allow comparison of the photometry between fields. The underlying image in Figure 1 is taken from the Digitized Sky Survey.

[1] Visiting Astronomer, Cerro Tololo Inter-American Observatory. CTIO is operated by AURA, Inc., under contract to the National Science Foundation.
[2] Present address: Department of Astrophysics, Planetary and Atmospheric Science, University of Colorado, Boulder, CO 80309; Henry.Throop@Colorado.edu.
[3] Present address: Department of Astronomy, University of Maryland, College Park, MD 20742; gwalker@astro.umd.edu.

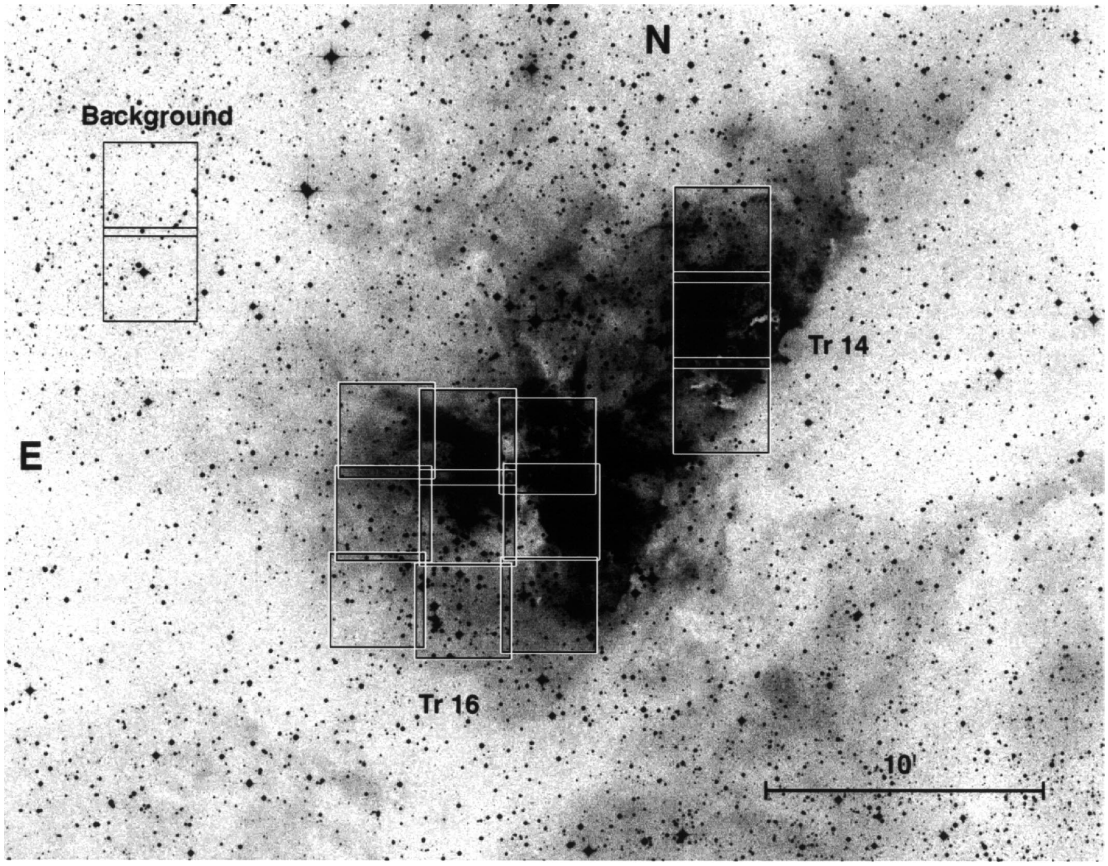

FIG. 1.—Observed fields for Tr 16, Tr 14, and the background. The image is taken from the STScI Digitized Sky Survey and centered on $\alpha_{2000} = 10^h44^m40^s$, $\delta_{2000} = -59°38' 00''$ with a width of 40′ and a height of 31′.

For each field we obtained three exposures (short, medium, and long) for each of the three filters. The typical seeing was 1.″5. The usual exposure times were 5, 40, and 400 s for the B and V filters, and 20, 150, and 1500 s for U. The short exposures were not needed for a few frames in which there were no bright stars to saturate. A few of the stars in the field were too bright even for 1 s exposures; as noted below, magnitudes for these stars were garnered from the literature. At the faint end, the errors became unacceptably large at $V \approx 19$. In total, about 120 separate images were reduced separately. In addition, about 60 sets of UBV observations were made of eight different Landolt (1983) standards over the course of five nights of observing.

The bias and flat-fielding were performed using CCDPROC within IRAF. Point spread function photometry was done on the program stars using the program DoPHOT, provided by P. Schechter (Schechter, Mateo, & Saha 1993). Aperture corrections were determined for each frame to tie the magnitudes from DoPHOT's square apertures into the magnitudes determined from IRAF APPHOT's circular apertures used on the standard stars. In Figure 2 we present the internal photometric uncertainties for individual measurements of V, $B-V$, and $U-B$ as a function of apparent V magnitude.

The transformation equations for the circular apertures were determined using IRAF's PHOTCAL package. First zero points, color terms, and extinction coefficients were derived for each night separately. Next we assumed that only the extinction would actually change from night to night and set the zero points and color terms equal to their average values and re-solved for the extinction coefficients for each night.

Given the different exposures and slightly overlapping frames, more than 60% of the stars were measured twice, and many were measured three or more times. The magnitudes were combined using a weighted average, where the relative weights were determined from the photometric uncertainties given by DoPHOT. Thus, for most stars, the formal uncertainties are very likely less than that shown in Figure 2. All the observations for each star were matched by their pixel coordinates using a matching program which started with the pixel offsets between frames. All discrepancies between magnitudes on different frames were flagged and examined individually for problems. Typical problems were caused by a star being too close to the edge of the frame on one image but not on another, or by a star on one frame being too close to a saturated object. The final output files contain 563 stars in Tr 16, and 290 stars in Tr 14. Some stars were too red for a good signal-to-noise measurement for U; for these stars, we present only B and V.

Tables 1 and 2 present the new photometry and new astrometric positions for J2000 as described below in § 2.4. The full tables are available electronically; only samples of the data are presented here. Table 3 presents cross-identifications for some of the stars.

2.2. *Comparison with Existing Photometry*

Figure 3 compares our photometry to the photoelectric photometry of Feinstein, Marraco, & Muzzio (1973) (*crosses*) and to the CCD photometry of Massey & Johnson

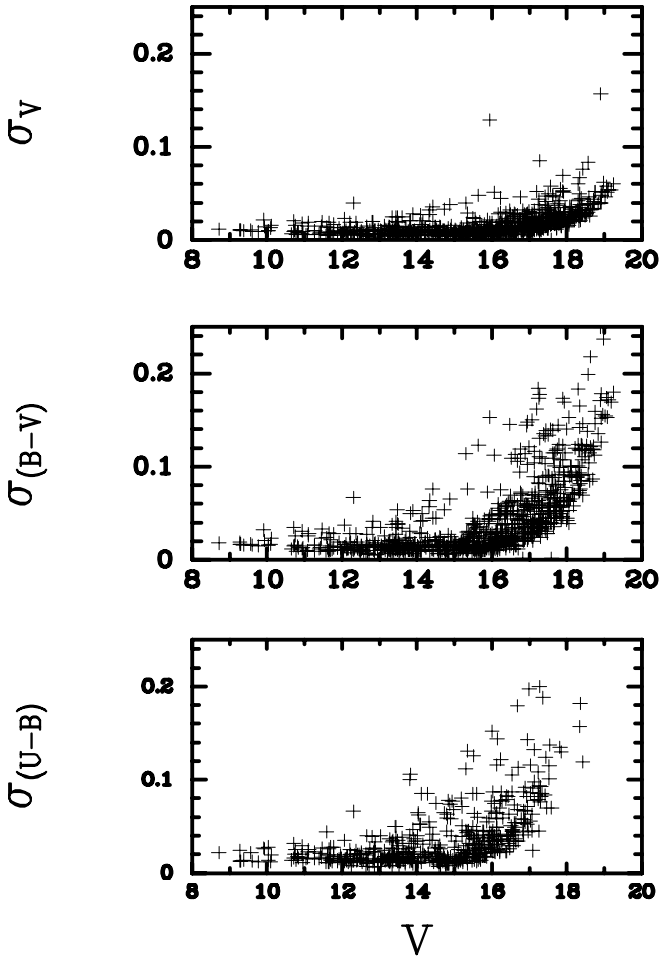

FIG. 2.—Internal photometric uncertainties σ for individual measurements as a function of apparent V magnitude for V magnitude, $B-V$ color, and $U-$B color. These uncertainties are produced by DoPHOT and represent the contributions from the photon statistics and the PSF fitting. We have not included here the uncertainties contributed by the transformation to the standard magnitude system (cf. Fig. 3). Since more than 60% of the stars were measured twice, the formal uncertainties per star are typically less than those shown.

TABLE 1

TRUMPLER 14: NEW PHOTOMETRY AND ASTROMETRIC POSITIONS FOR J2000[a]

R.A.	Decl.	V	$B-V$	$U-B$
10 43 38.19.....	−59 34 41.9	16.24	0.94	
10 43 38.73.....	−59 34 44.6	12.13	0.42	
10 43 38.88.....	−59 33 01.9	16.26	1.12	
10 43 38.98.....	−59 33 50.0	17.14	1.40	
10 43 39.00.....	−59 31 16.5	18.05	0.92	
10 43 39.03.....	−59 29 34.8	16.14	0.96	0.80
10 43 39.06.....	−59 31 02.9	17.08	0.97	
10 43 39.10.....	−59 33 31.1	16.27	0.79	0.29
10 43 39.15.....	−59 29 22.5	11.27	1.33	1.04
10 43 39.21.....	−59 34 48.7	15.68	1.29	

[a] The full designation of a star in this table, as recommended by the IAU, is Tr 14: DETWC JHHMMSS.S ± DDMMSS, where the coordinates have been *truncated*, not rounded. The acronym "DETWC" indicates the authors, and the prefix "J" indicates that the coordinates are for J2000. This table is available in its entirety as a machine-readable table in the electronic edition of *The Astrophysical Journal*.

TABLE 2

TRUMPLER 16: NEW PHOTOMETRY AND ASTROMETRIC POSITIONS FOR J2000[a]

R.A.	Decl.	V	$B-V$	$U-B$
10 44 27.92.....	−59 45 21.6	10.11	0.91	0.64
10 44 28.07.....	−59 44 17.0	15.37	0.68	0.34
10 44 28.25.....	−59 43 47.3	12.28	0.18	
10 44 28.28.....	−59 40 16.2	12.31	0.28	0.09
10 44 28.67.....	−59 41 45.1	16.87	1.44	
10 44 28.77.....	−59 44 02.0	13.47	0.25	
10 44 28.90.....	−59 37 10.4	15.33	0.94	
10 44 29.04.....	−59 43 47.6	12.42	0.16	
10 44 29.07.....	−59 42 34.9	12.08	0.14	
10 44 29.26.....	−59 41 43.4	15.21	1.20	0.29

[a] The full designation of a star in this table, as recommended by the IAU, is Tr 16: DETWC JHHMMSS.S ± DDMMSS, where the coordinates have been *truncated*, not rounded. The acronym "DETWC" indicates the authors, and the prefix "J" indicates that the coordinates are for J2000. This table is available in its entirety as a machine-readable table in the electronic edition of *The Astrophysical Journal*.

(1993) (*circles*). The difference in V, $B-V$, and $U-B$ (in the sense of ours minus theirs) is plotted as a function of apparent V magnitude. Massey & Johnson (1993) used the same CTIO U filter that we did, but calibrated their photometry using Feinstein's magnitudes for cluster stars rather than the Landolt standards. Although the average differences for V and $B-V$ are not significantly different from zero, our $U-B$ colors are bluer than Feinstein's by 0.09 ± 0.02 (standard error), and bluer than Massey and Johnson's by 0.08 ± 0.03.

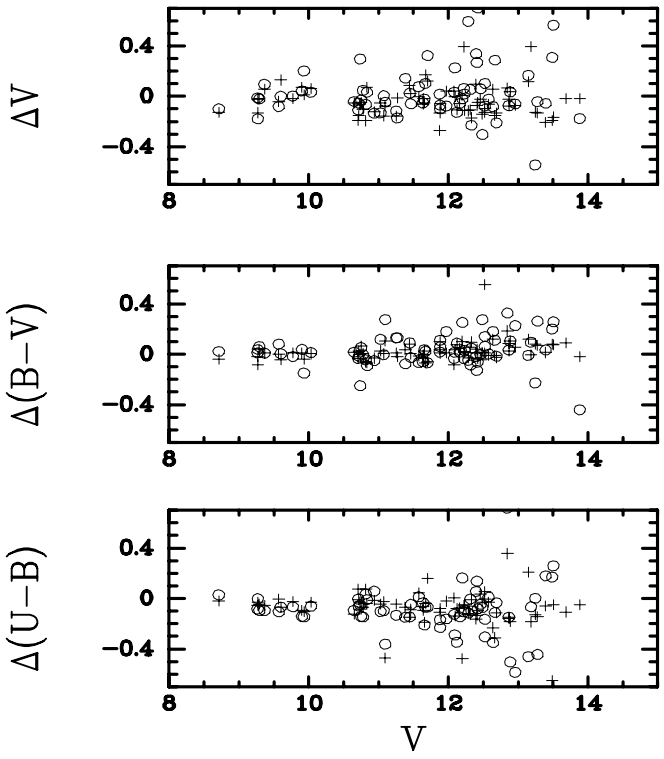

FIG. 3.—Comparison of the new photometry to the photoelectric photometry of Feinstein et al. (1973) (*crosses*) and to the CCD photometry of Massey & Johnson (1993) (*circles*). The differences ΔV, $\Delta B-V$ and $\Delta U-B$, all in the sense of ours minus theirs, are shown as a function of apparent V magnitude.

TABLE 3

CROSS-IDENTIFICATIONS FOR SOME STARS

New Designation[a]	Feinstein et al. 1973	Massey & Johnson 1993	Other[b]
Tr 14: DETWC J104339.1−592922.....		82	
Tr 14: DETWC J104341.2−593552.....		91	
Tr 14: DETWC J104343.6−593403.....	14–28	99	
Tr 14: DETWC J104348.7−593324.....	14–21	127	Y547
Tr 14: DETWC J104348.8−593335.....	14–22	128	
Tr 14: DETWC J104350.8−593152.....		203	Y611
Tr 14: DETWC J104353.6−593328.....	14–5	150	Y550
Tr 14: DETWC J104355.1−593159.....	14–14	160	
Tr 14: DETWC J104355.2−593239.....	14–10	161	
Tr 14: DETWC J104355.2−593315.....	14–4	163	Y551
Tr 14: DETWC J104356.1−593441.....	14–26	170	
Tr 14: DETWC J104356.2−593228.....	14–11	168	
Tr 14: DETWC J104357.2−593208.....	14–13	174	
Tr 14: DETWC J104357.6−593338.....	14–6	178	Y530
Tr 14: DETWC J104358.0−593231.....	14–12		
Tr 14: DETWC J104358.0−593354.....	14–18		
Tr 14: DETWC J104359.5−593231.....	14–7	189	
Tr 14: DETWC J104359.9−593147.....	14–15	191	
Tr 14: DETWC J104359.9−593311.....		194	Y553
Tr 14: DETWC J104400.7−593152.....	14–16	196	
Tr 14: DETWC J104401.0−593546.....	16–127	200	
Tr 14: DETWC J104402.7−593228.....	14–17		
Tr 16: DETWC J104428.2−594347.....	16–61	324	
Tr 16: DETWC J104428.2−594016.....	16–58	313	
Tr 16: DETWC J104429.0−594347.....	16–60	318	
Tr 16: DETWC J104429.0−594234.....	16–18		
Tr 16: DETWC J104429.5−593837.....	16–12	321	
Tr 16: DETWC J104430.4−593726.....	16–10	327	
Tr 16: DETWC J104430.6−594140.....	16–17	329	
Tr 16: DETWC J104433.0−594026.....	16–13	339	
Tr 16: DETWC J104433.7−593820.....	16–79	341	
Tr 16: DETWC J104434.2−594309.....	16–62	345	
Tr 16: DETWC J104437.2−594001.....	16–14	357	
Tr 16: DETWC J104438.3−594306.....	16–63	363	
Tr 16: DETWC J104440.4−594149.....	16–16	370	
Tr 16: DETWC J104440.9−594321.....	16–49		
Tr 16: DETWC J104441.0−594010.....	16–15	372	
Tr 16: DETWC J104442.8−593807.....	16–45	378	
Tr 16: DETWC J104445.1−594325.....	16–48	393	
Tr 16: DETWC J104446.0−594029.....	16–43	395	
Tr 16: DETWC J104447.1−593920.....	16–44	399	
Tr 16: DETWC J104453.8−593748.....	16–29	424	
Tr 16: DETWC J104456.6−594024.....	16–41	445	
Tr 16: DETWC J104456.7−594003.....	16–40	446	
Tr 16: DETWC J104457.5−593639.....	16–30	450	
Tr 16: DETWC J104457.9−594000.....	16–39	453	
Tr 16: DETWC J104458.9−594223.....	16–46	457	
Tr 16: DETWC J104500.2−594005.....	16–38	461	
Tr 16: DETWC J104500.3−594334.....	16–25		
Tr 16: DETWC J104503.1−594013.....	16–8	467	
Tr 16: DETWC J104505.0−594207.....	16–75		
Tr 16: DETWC J104505.2−594142.....	16–72	477	
Tr 16: DETWC J104505.7−594124.....	16–68	479	
Tr 16: DETWC J104505.8−594519.....	16–23	484	
Tr 16: DETWC J104505.9−594307.....	16–9	481	
Tr 16: DETWC J104505.9−594418.....	16–24	483	
Tr 16: DETWC J104506.1−594112.....	16–67		
Tr 16: DETWC J104507.1−594058.....	16–77	489	
Tr 16: DETWC J104507.9−594134.....	16–69	491	
Tr 16: DETWC J104507.9−593902.....	16–51	490	
Tr 16: DETWC J104508.4−593848.....	16–52	492	
Tr 16: DETWC J104508.9−594041.....	16–37	495	
Tr 16: DETWC J104509.3−594128.....	16–70	498	
Tr 16: DETWC J104509.6−594009.....	16–33	499	
Tr 16: DETWC J104509.8−594257.....	16–74		

TABLE 3—*Continued*

New Designation[a]	Feinstein et al. 1973	Massey & Johnson 1993	Other[b]
Tr 16: DETWC J104510.6−593856.....	16–53		
Tr 16: DETWC J104511.2−594111.....	16–2	506	
Tr 16: DETWC J104512.3−594500.....		512	HD93343
Tr 16: DETWC J104512.7−593906.....	16–54	511	
Tr 16: DETWC J104512.8−594446.....	16–34	516	BD −59 2635
Tr 16: DETWC J104512.9−594419.....	16–110	517	BD −59 2636
Tr 16: DETWC J104516.5−593957.....	16–27	533	
Tr 16: DETWC J104516.6−594337.....	16–112	535	BD −59 2641
Tr 16: DETWC J104519.4−593937.....	16–55	547	

[a] See the footnotes to Tables 1 and 2 for a description of the designation.
[b] A "Y" designation refers to the numbering in Cudworth et al. 1993.

Some of the variations in U measurements are unavoidable, due to the nature of the spectral energy distributions of the standards. Most of the Landolt (1983) standards in this color range are probably A through F stars, not highly reddened O and B stars. In addition, U filters can be quite different from the "standard," making transformations difficult. We discuss this issue again below, when considering the reddening.

2.3. *Existing Proper Motions and Spectroscopy*

Cudworth et al. (1993) determined proper motions and cluster membership probabilities for nearly 600 stars in the η Carinae region, to a limiting magnitude of approximately $V \approx 15.5$. These stars belonged primarily to Tr 16, Tr 14, and Cr 232. After identifying many stars in common between the proper motion sample and the current sample, we were able to determine a transformation between the coordinate system of Cudworth et al. (1993) and the instrumental coordinates, thus allowing us to match up the membership probabilities with all the stars in common between the two samples.

Spectra were available for the brightest of the stars from a variety of sources. Spectral classifications from Walborn (1971), Walborn (1973), Morrell, Garcia, & Levato (1988), and Massey & Johnson (1993) were all used in the distance determination discussed in § 3.1. The sample of stars used to determine the distance are presented in Table 4. Table 5 contains the spectral types used for the very brightest stars, which were saturated on our frames, as well as the sources of those spectral types.

2.4. *New Astrometry*

Astrometric positions for J2000 were derived relative to the *HST* Guide Star Catalog for all the program stars using TFINDER within IRAF at NOAO. Each frame was measured separately, and multiple determinations for a single star

TABLE 4

STARS USED FOR SPECTROSCOPIC PARALLAX

Star[a]	P	Spectral Type	Ref.[b]	V	$B-V$	M_V	$(B-V)_0$	A_V	V_0-M_V
14–20	96	O6 V((f))	W	9.57	0.28	−5.1	−0.32	1.92	12.75
14–6	94	B1 V	M	11.08	0.20	−3.2	−0.26	1.46	12.81
14–4	97	B0 V	M	11.03	0.27	−3.8	−0.30	1.81	13.01
14–21	81	O9 V	M	10.78	0.35	−4.4	−0.31	2.10	13.08
14–22	94	B2 V	MJ	12.23	0.34	−2.5	−0.24	1.86	12.87
16–127.....	96	O9 V	MJ	10.65	0.37	−4.4	−0.31	2.16	12.89
16–8	96	B0.5 V	MJ	10.71	0.10	−3.8	−0.28	1.23	13.28
16–72	95	B1 V	MJ	12.10	0.28	−3.2	−0.26	1.71	13.58
16–33	86	B2 V	MJ	12.22	0.29	−2.5	−0.24	1.69	13.04
16–16	95	B1 V	MJ	10.72	0.26	−3.2	−0.26	1.67	12.24
16–13	95	B1 V	MJ	10.83	0.15	−3.2	−0.26	1.31	12.72
16–17	96	B1 V	MJ	10.82	0.18	−3.2	−0.26	1.40	12.62
16–15	96	B0 V	MJ	11.27	0.39	−3.8	−0.30	2.20	12.86
BD −59 2641.....	96	O6 V((f))	MJ	9.27	0.30	−5.1	−0.32	1.99	12.38
BD −59 2636.....	96	O8 V	W	9.29	0.35	−4.6	−0.31	2.11	11.78
BD −59 2635.....	96	O8.5 V	MJ	9.36	0.24	−4.9	−0.31	1.75	12.51
HD 93343.....	96	O7 V(n)	W	9.60	0.24	−4.9	−0.32	1.80	12.69
16–9	95	O9.5 V	MJ	9.77	0.24	−4.0	−0.30	1.73	12.04
16–74	96	B1 V	MJ	11.64	0.24	−3.2	−0.26	1.60	13.24
16–24	96	B2 V	MJ	11.58	0.14	−2.5	−0.24	1.29	12.85
16–55	96	B1.5 V	MJ	12.16	0.28	−2.8	−0.25	1.68	13.28
16–10	96	B0 V	MJ	9.90	0.31	−3.8	−0.30	1.95	11.76
16–14	96	B0.5 V	MJ	11.67	0.35	−3.8	−0.28	2.03	13.45
16–18	96	B2 V	MJ	12.08	0.14	−2.5	−0.24	1.23	13.35

[a] Stars which are from neither the HD nor BD catalog are referred to by their numbering designated in Feinstein et al. 1973.
[b] "W" indicates Walborn 1973, "M" indicates Morrell et al. 1988, and "MJ" indicates Massey & Johnson 1993.

TABLE 5

SATURATED STARS TAKEN FROM THE LITERATURE

Star	Spectral Type	Reference
HD 93129AB	O3 If	1
HD 93205	O3 V	1
HDE 303308	O3 V((f))	1
HD 93204	O5 V((f))	1
BD −59 2603.....	O7 V((f))	1
η Carinae		2

REFERENCES.—(1) Walborn 1973; (2) Davidson et al. 1986 and Westphal & Neugebauer 1969.

were averaged. Discrepancies were flagged and examined individually. All the reference stars used were from a single plate, GSC plate 06A6. Unfortunately, the northwest frame in the Tr 16 mosaic did not contain any GSC stars due to the heavy nebulosity in that area. However, there were stars from the original Cudworth et al. (1993) sample on the northwest frame. Thus, we tied the stars on the northwest frame into the original astrometric system used by Cudworth et al. (1993) and then tied that system into the GSC system. The rms uncertainties for all the derived coordinates are less than 0.″2. The coordinates for each star are included in Tables 1 and 2.

3. ANALYSIS

3.1. *Reddening and Distance*

We used two different methods to determine values of the reddening for individual stars. For the stars with spectra, we compare their observed colors to the intrinsic colors tabulated by Fitzgerald (1970). For stars with photometry only we calculated the reddening-free parameter $Q = (U-B) - m(B-V)$, where m is the slope of the reddening curve, $E(U-B)/E(B-V)$. For early-type stars with $(B-V) \approx 0$, the average galactic value of m is 0.72 (Sharpless 1963). Using stars with both photometry and spectroscopy, we find a value for m of 0.63 ± 0.02. Massey & Johnson (1993) obtained a value of 0.73 ± 0.01 for this same region.

Either our $U-B$ colors are off (bluer than Feinstein's by 0.09 ± 0.02, using a sample of 71 stars) and the reddening slope is normal, or the colors are correct and the reddening slope is shallower than average. Whether or not the extinction in the Eta Carinae region is anomalous has been under discussion for quite some time, e.g., Herbst (1976), Turner & Moffat (1980), Tapia et al. (1988), and Marraco, Vega, & Vrba (1993), to name only a few. Tapia et al. (1988) find a *foreground* value for $R = A_V/E(B-V)$ of 3.2. We do not have enough wavelength coverage to determine R for ourselves. With insufficient data to solve this problem completely, we use $m = 0.63$, with the idea that even if the photometry is too blue, this combination will produce dereddened colors consistent with standard colors. We also use $R = 3.2$. The fact that the resulting data seem to fit the theoretical evolutionary tracks quite well indicates that, at the very least, this combination of parameters gives a consistent solution.

For stars without spectral types we calculated the reddening-free parameter Q and compared it to Q computed for standard colors as a function of spectral type, thus revealing the intrinsic colors of the star. However, this process only works for stars with $Q < -0.4$, or $T_{\rm eff} >$ 15,000 K on the main sequence. For stars cooler than this, Q becomes degenerate with spectral type. Thus, we could only determine individual reddenings for the bluest stars. This method was used in both the cluster fields and in the background field.

We now combine these two methods for determining individual reddenings for stars with the membership probability information provided by the proper motion study of Cudworth et al. (1993). Figures 4*a* and 4*b* compare the number of stars as a function of $E(B-V)$ for both Tr 16 and Tr 14, distinguishing between cluster members (*solid lines*) and stars with no measurement of membership probability (*dashed lines*), where stars with membership probability $P \geq 0.8$ are considered members. Figure 4*c* shows the distribution of stars in Tr 16 which are considered certain nonmembers, i.e., stars with membership probability $P < 0.20$. (An equivalent figure is not shown for Tr 14 because there were virtually no stars with measured probabilities this low.) Finally, Figure 4*d* shows the distribution of color excesses for all stars in the background field which have individual reddenings.

Inspection of Figure 4 reveals that known members cluster around an average color excess of $E(B-V) = 0.6$ for both regions, whereas the known nonmembers in Tr 16 cluster around 1.0, and the background stars cluster around an average value closer to 1.2. The stars *without* membership probabilities in Tr 16 show a roughly bimodal distribution with peaks around those same values of 0.6 and 1.2. We interpret this bimodal distribution as the overlap of the member and nonmember distributions.

The median color excess for the 34 stars in the background field is $E(B-V) = 1.22$. As seen in Figure 4*d*, only two of these stars have $E(B-V) < 0.9$. Thus, we believe that most of the stars in the cluster fields with $E(B-V) > 0.9$ are actually not cluster members and have discarded these stars from all future diagrams. This process very nicely removed several stars that were in unphysical places on the H-R diagram.

Most stars were too red to be able to use Q to calculate an individual reddening. For these stars we have assumed a reddening equal to the average for members. The values used were a median $E(B-V) = 0.58$ for Tr 14 (derived from 15 stars), and 0.64 for Tr 16 (derived from 43 stars). Without membership information, these average values would have been much higher.

We used spectroscopic parallax to determine the distance modulus, using only the 24 stars with spectra and with membership probability $P \geq 80$ in Tr 14 and Tr 16 combined. Table 4 contains the stars that were used, their spectral types from the literature, their observed V and $B-V$, and the M_V and $(B-V)_0$. The calibration of M_V with spectral type was taken from Conti et al. (1983) for the O stars, and Humphreys & McElroy (1984) for the B stars. As before, the calibration of $(B-V)_0$ with spectral type was taken from Fitzgerald (1970). The distance modulus obtained with these stars was $(m-M)_0 = 12.79 \pm 0.10$ (standard error).

This restriction to stars with highly probable membership resulted in a very different result from that of Massey & Johnson (1993). In comparison, they used 48 stars and the method of spectroscopic parallax to derive a distance modulus of 12.55 ± 0.08 over the entire area. Other recent determinations of the distance modulus include determinations of 12.50 ± 0.20 for Tr 14 by Vazquez et al. (1996),

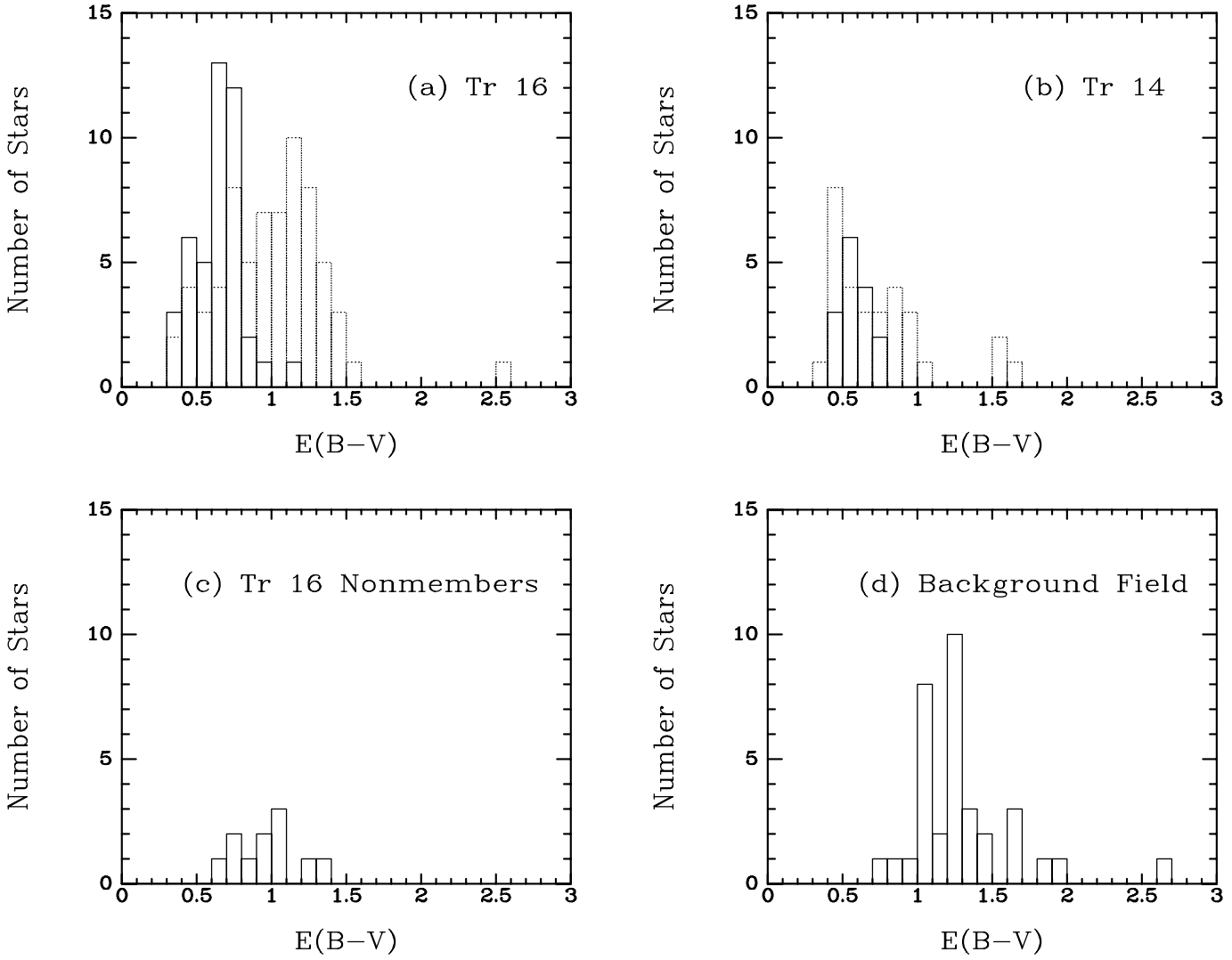

FIG. 4.—Distribution of reddening for individual stars. In (*a*) and (*b*), the solid lines represent the histograms for stars which are known members of Tr 16 and Tr 14, respectively. The dashed lines represent the histograms for stars which had no probabilities measured. In (*c*) we show the histogram for stars in Tr 16 known to be nonmembers, and in (*d*) the distribution for stars measured in the background field.

and 12.0 $\pm$ 0.2 for Tr 16 by Tapia et al. (1988), both derived from main-sequence fitting. The early spectroscopic parallax by Walborn (1973) gave distance moduli of 12.72 for Tr 14 (five stars), and 12.11 for Tr 16 (nine stars). In this paper we use our derived distance modulus of 12.79 in all our calculations.

Figures 5*a* and 5*b* present dereddened color-magnitude diagrams for Tr 16 and Tr 14. The symbols are described in the figure captions. Table 5 contains the list of stars which were saturated on our frames, and thus taken from the literature.

3.2. *Transformation to the Theoretical H-R Diagram*

The stars were transformed from the observational color-magnitude diagram to the theoretical H-R diagram. For stars with spectra, the calibration of effective temperature and bolometric correction with spectral type was taken from Chlebowski & Garmany (1991) for the O stars, and Humphreys & McElroy (1984) for the later stars. The transformations based purely on photometry depended on the color of the star and are detailed in Table 7 of Massey et al. (1995).

Figure 6 plots our data for Tr 16, Tr 14, and the background field on top of the evolutionary tracks of Schaller et al. (1992). The tracks are those using convective overshoot and a standard mass loss rate, for an abundance of $Z = 0.020$. The tracks are plotted as thin solid lines and are labeled in solar masses. The various stellar symbols are described in the figure captions. Following Massey & Johnson (1993), we have also placed η Carinae on the diagram using the effective temperature of Davidson et al. (1986) and the bolometric luminosity, corrected for the difference in assumed distance, of Westphal & Neugebauer (1969).

3.3. *The Stellar Birthline*

The stellar birthline marks the set of points in the H-R diagram where stars first appear at optical wavelengths, at the end of their accretion phase (see Palla & Stahler 1990, and Palla & Stahler 1992). Figure 6 plots the theoretical stellar birthline of Palla & Stahler (1993) for intermediate-mass stars as a thick solid line, and the stellar birthline of Beech & Mitalas (1994) as a dashed line. In Tr 16 the birthline of Palla & Stahler (1993) much more closely follows the

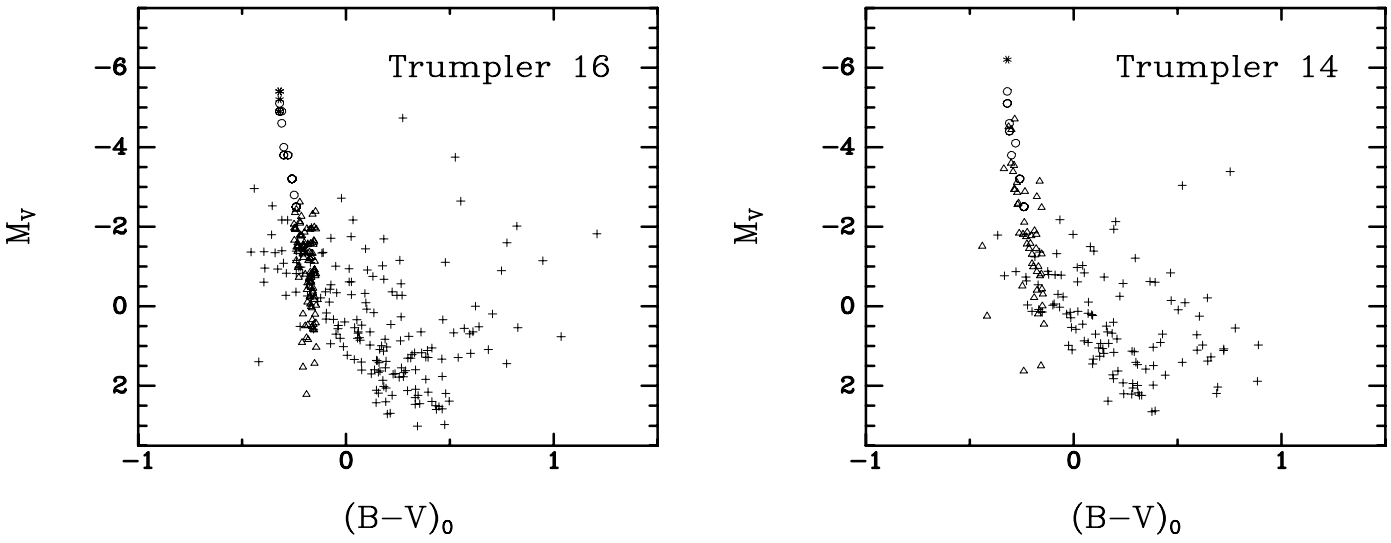

FIG. 5.—Dereddened color-magnitude diagrams for (*a*) Tr 16 and (*b*) Tr 14. The few stars with known spectral types are represented by circles. Stars with their reddenings individually derived from the reddening-free parameter *Q* are shown as triangles, and stars given an average reddening are represented by crosses. Stars denoted with asterisks were saturated on our frames and have been taken from the literature.

upper envelope of the distribution of stars, and in fact matches the data remarkably well. The model and data do not agree as closely in Tr 14 but are still consistent with each other.

Why do we believe that the stars under the birthline are in fact pre–main-sequence stars, and not foreground or background stars? To begin with, the edge of the distribution of stars lines up nicely with the ZAMS, which would

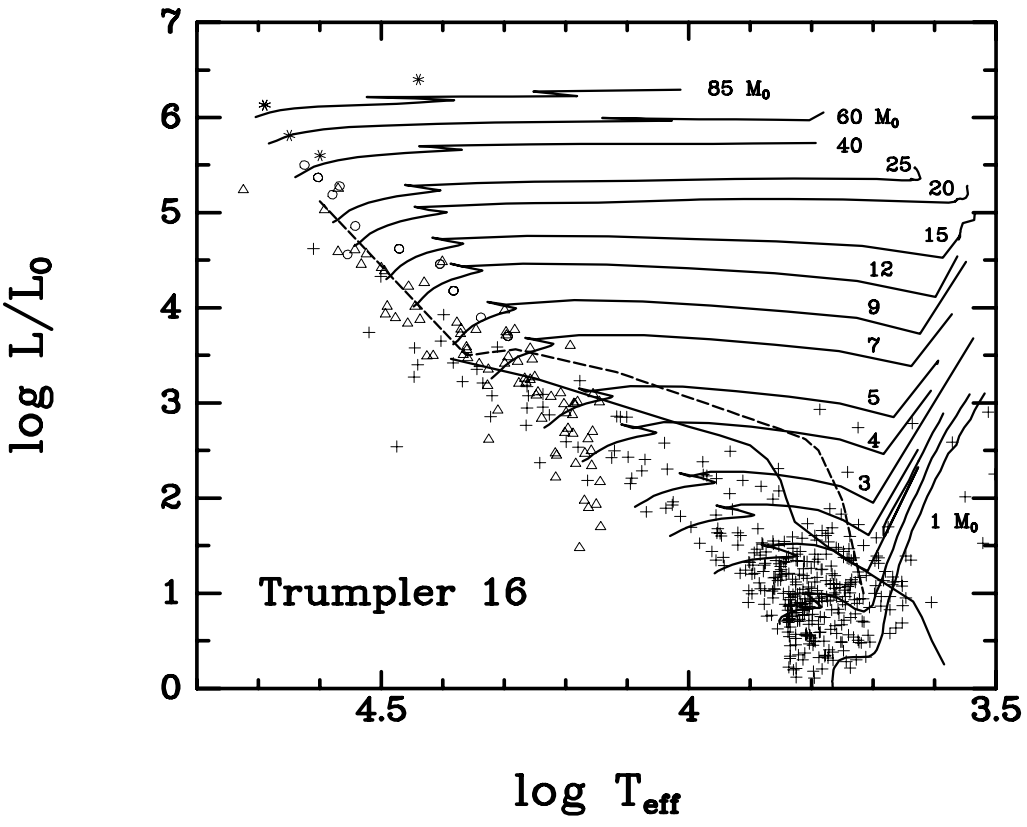

FIG. 6*a*

FIG. 6.—Theoretical H-R diagrams for (*a*) Tr 16, (*b*) Tr 14, and (*c*) the background field. Stars with their reddening derived from their known spectral class are represented by circles, with their reddening individually derived from Q are shown as triangles, and stars given an average reddening are represented by crosses. Stars denoted with asterisks were saturated on our frames and have been taken from the literature. The light solid lines are post–main-sequence evolutionary tracks taken from Schaller et al. (1992), with the appropriate masses labeled in solar masses. The dark solid line is the stellar birthline of Palla & Stahler (1993), while the dashed line is the stellar birthline of Beech & Mitalas (1994). Some of the tracks have been truncated to avoid confusion due to overlapping.

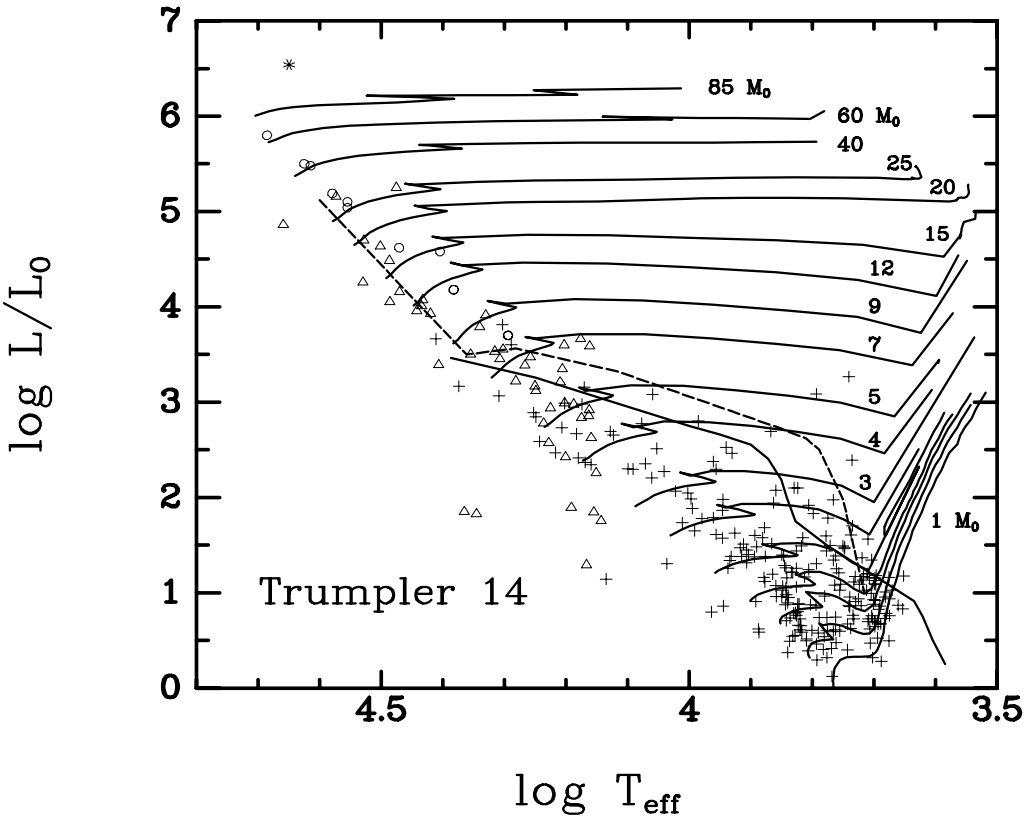
log L/L$_0$
85 M$_0$
60 M$_0$
40
25
20
15
12
9
7
5
4
3
1 M$_0$
Trumpler 14
log T$_{eff}$

FIG. 6*b*

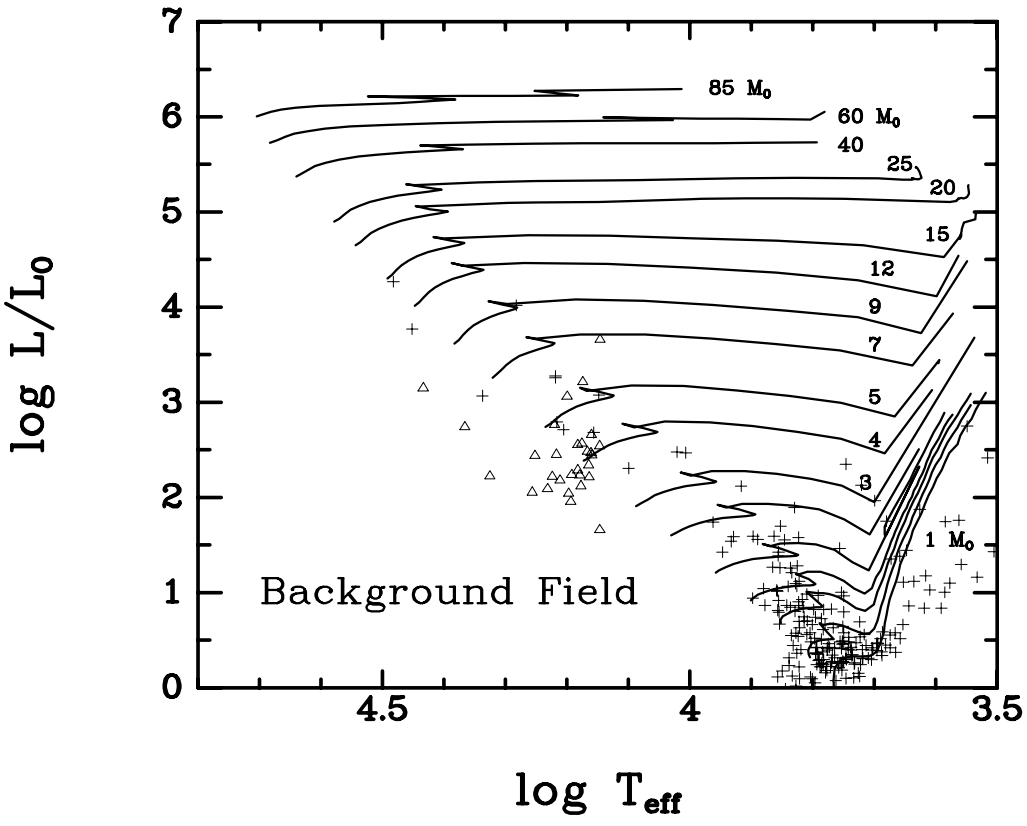
log L/L$_0$
85 M$_0$
60 M$_0$
40
25
20
15
12
9
7
5
4
3
1 M$_0$
Background Field
log T$_{eff}$

FIG. 6*c*

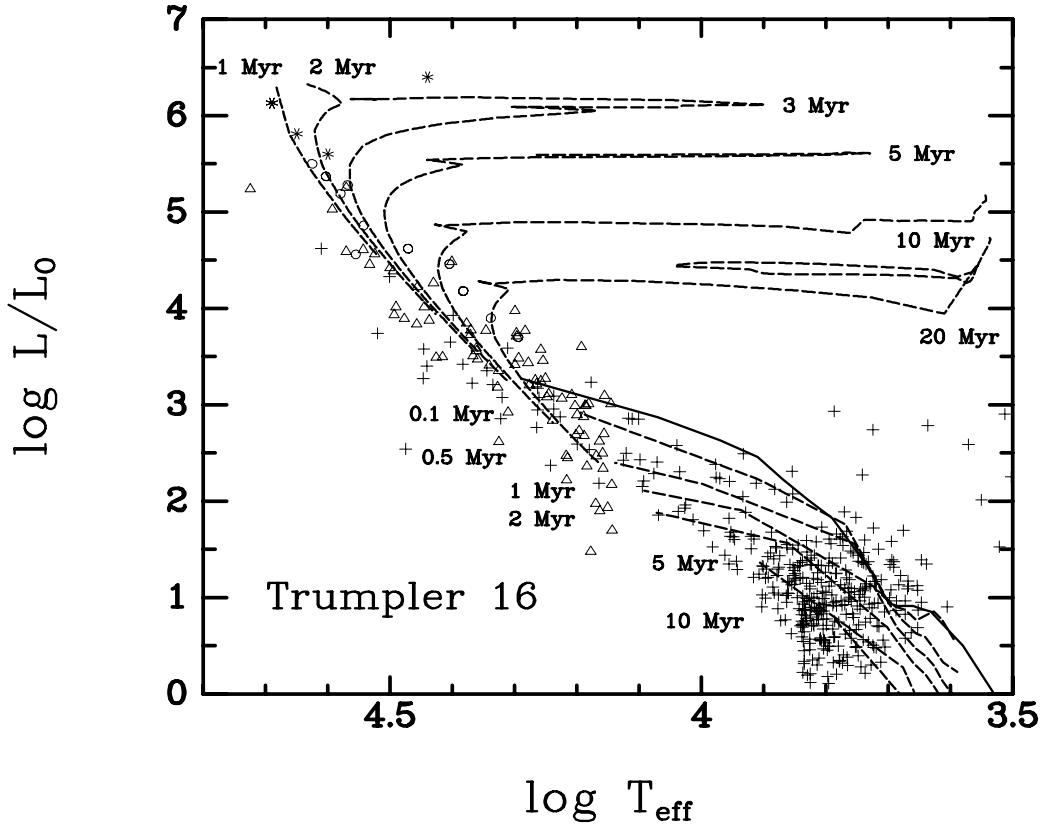

FIG. 7*a*

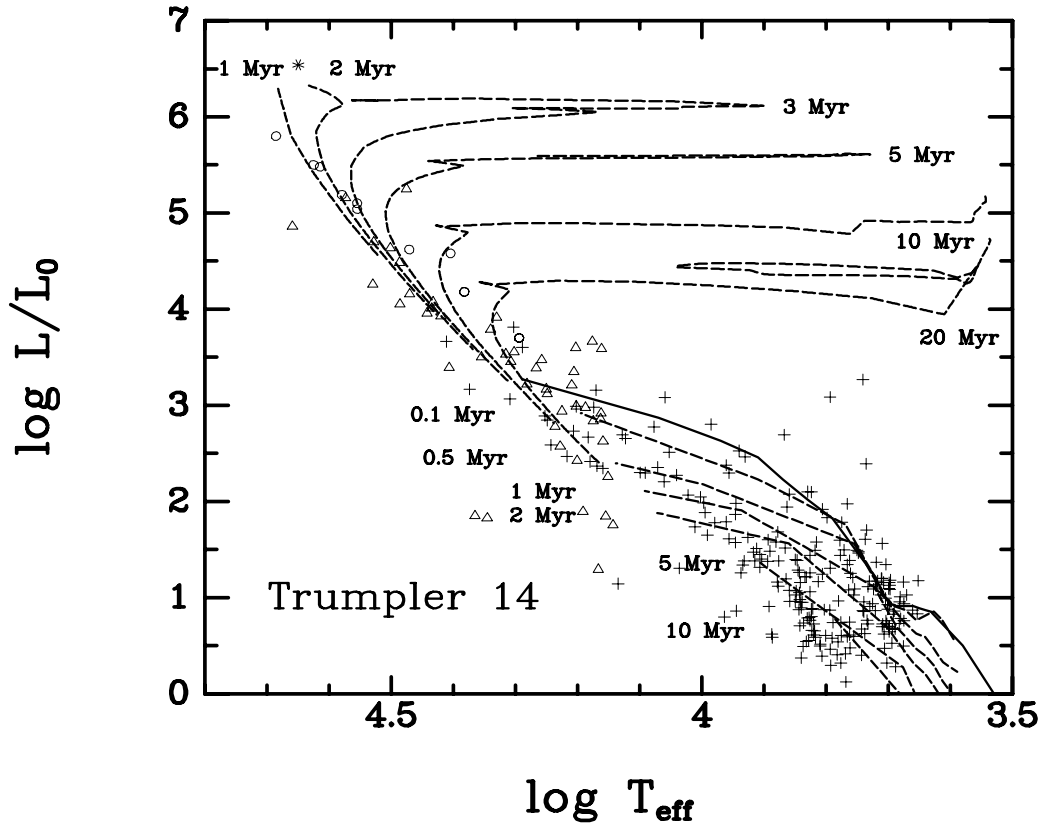

FIG. 7*b*

FIG. 7.—Theoretical H-R diagrams for (*a*) Tr 16 and (*b*) Tr 14, with isochrones labeled in years. The post–main-sequence isochrones are from the evolutionary tracks of Schaller et al. (1992), while the pre–main-sequence isochrones are derived from the models of Palla & Stahler (1993). The heavy solid line is again the stellar birthline of Palla & Stahler (1993).

not be expected if the stars were at different distances. Next consider Figure 6*c*, which is an H-R diagram for the stars from the background field. For stars too red to use Q, i.e., $Q > -0.4$, the average reddening for Tr 16 members has been applied. In this figure, the few stars below the main sequence are the stars which have been individually dereddened. They appear to be blue background stars. The few stars to the right of the evolutionary tracks shown, at about $\log T_{\rm eff} \approx 3.6$ and $\log L/L_{\odot} \approx 1$, are most likely foreground stars. However, the bulk of the stars in the background field are clumped and are amazingly close together in the H-R diagram for stars which all have different distances. Some may be foreground stars which have been slightly overcorrected for reddening, but it seems that most of these stars represent a low-mass, wide-spread population which is at the same distance as the clusters in question, and not a traditional background in the sense of having random distances. This local background population is centered at a place under the birthline both cooler and less luminous than most of the stars detected in Tr 14 or 16. Thus, the stars in Tr 14 and 16 really do seem to be a population separate from that of the local background.

3.4. *The Age Spread*

Figure 7 plots post–main-sequence isochrones from the same evolutionary tracks described above. G. Meynet kindly provided the data tables for the evolutionary tracks, and a program which extracts an isochrone from those data. The isochrones are plotted as thin dashed lines and are labeled with the age in years. In Figure 7 we have also added pre–main-sequence (PMS) isochrones derived from the evolutionary tracks of Palla & Stahler (1993).

Inspection of the diagram for Tr 16 shows immediately that it is populated by stars of very different ages. The most massive stars are represented at ages of 1 Myr, 2 Myr, and, if we believe the placement of η Carinae, 3 Myr. There are a couple of 30–35 $M_{\odot}$ stars also on the 3 Myr isochrone, and a 16–17 $M_{\odot}$ star at about 6 Myr. Other than this last star, there appear to have been no massive stars formed between 3 and 10 Myr ago. However, if we have corrected for background stars correctly, there are many PMS stars present from as old as 10 Myr to as young as 0.1 Myr. Thus, we conclude that *intermediate-mass* star formation has proceeded continuously in Tr 16 over the past 10 Myr, whereas the high-mass stars were formed within the last 3 Myr, with only one apparent exception. Thus, the formation of the intermediate-mass stars (down to $\approx 1\ M_{\odot}$) started long before the OB stars formed, and apparently has not been disrupted by the formation of those same OB stars.

The diagram for Tr 14 is similar. With the exception of one 25 $M_{\odot}$ star on the 5 Myr isochrone, there appear to have been no massive stars formed between 2 and 10 Myr ago. Again, if we have corrected for background stars correctly, there are PMS stars present ranging in age from 0.1 to 10 Myr.

This observation of continuous star formation does not support the picture of ongoing formation of low-mass stars being truncated by the formation of any high-mass stars, first suggested by Herbig (1962) from his observations of Hyades and Pleiades, and described theoretically by Norman & Silk (1980). The seminal paper by Herbst & Miller (1982) describes an age spread of 20 ± 10 Myr in NGC 3293 and suggests that the formation of high-mass stars terminates the star formation process. This age spread is comparable to what we see in Tr 14 and Tr 16. However, they did not have the PMS isochrones with which to determine whether the intermediate-mass star formation had been continuous.

Our results are reminiscent of those of Hillenbrand et al. (1993) for NGC 6611, who found the most massive stars to be about 2 Myr with an age spread of about 1 Myr. (They noted however, that if they allowed for an error of one spectral subtype, that their data could be consistent with *no* age spread—all the massive stars could have been born on "a particular Tuesday.") However, there was also evidence for an intermediate-mass PMS population with ages of 0.25–1 Myr, and one evolved star with an age of about 6 Myr. Thus, they also concluded that the "formation of O stars neither ushered in nor concluded the star formation process" in that young complex.

In another study of Tr 14, Vazquez et al. (1996) also found an age for the most massive stars of 1.5 ± 0.5 Myr. In addition they cite the "magnitude-spread at constant color" as evidence for continuous star formation over the last 5 Myr. Another very young cluster, NGC 2264, was similarly suspected of having a spread in formation time of roughly 10 Myr by Warner, Strom, & Strom (1977) due to the luminosity spread at constant color. More recently, Luhman et al. (1998) found an age spread from 0.5 to 10 Myr in IC 348, most of it in the last 3 Myr. However, Stauffer et al. (1998) could put only an upper limit of 20 Myr on the age spread for IC 2391 and IC 2602.

4. SUMMARY AND CONCLUSIONS

In this work we present new UBV CCD photometry and astrometry for over 850 stars in the very young clusters Trumpler 14 and 16. Including existing proper motions in the reddening analysis, we find that the "background" stars are much more highly reddened than the cluster stars, and therefore use the reddening to extend the determination of cluster membership many magnitudes fainter than the determination made astrometrically. Using existing spectra for as many stars as possible, we have mapped the color-magnitude diagrams into the theoretical H-R diagram.

We find two very interesting results: the first is that the theoretical stellar birthline of Palla & Stahler (1993) for intermediate-mass stars is a much better fit to the data than that of Beech & Mitalas (1994). In fact, the data in Tr 16 match the Palla & Stahler birthline remarkably well. In Tr 14, which contains fewer stars, the data are consistent with either model.

The second result is strong evidence for a significant age spread in both regions. Using the PMS isochrones of Palla & Stahler (1993), we find that Tr 14 and 16 have been forming intermediate-mass stars continuously over the last 10 Myr, whereas the high-mass stars formed only within the last 2–3 Myr. Each region seems to contain one exception, a star in the 5–6 Myr range. There is no evidence that the formation of the intermediate-mass stars was disrupted by the formation of high-mass stars.

We are grateful to P. Massey for his comments, R. Millis for his hospitality at Lowell during K. D. E.'s sabbatical when much of the analysis was performed, G. Meynet for the program which computes isochrones from his evolu-

tionary tracks, F. Palla for supplying digitized versions of his evolutionary tracks, an anonymous referee for useful comments, and P. Schechter for the use of DoPhot. H. T. and G. W. acknowledge the support of the NSF through the REU program at Northern Arizona University under NSF grant AST9200137.

REFERENCES

Beech, M., & Mitalas, R. 1994, ApJS, 95, 517
Chlebowski, T., & Garmany, C. D. 1991, ApJ, 368, 241
Conti, P. S., Garmany, C. D, deLoore, C., & Vanbeveren, D. 1983, ApJ, 274, 302
Cudworth, K. M., Martin, S. C., & DeGioia-Eastwood, K. 1993, AJ, 105, 1822
Davidson, K., Dufour, R. J., Walborn, N. R., & Gull, T. R. 1986, ApJ, 305, 867
Feinstein, A., Marraco, H. G., & Muzzio, J. C. 1973, A&AS, 12, 331
Fitzgerald, M. P. 1970, A&A, 4, 234
Herbig, G. H. 1962, ApJ, 135, 736
Herbst, W. 1976, ApJ, 208, 923
Herbst, W., & Miller, D. P. 1982, AJ, 87, 1478
Hillenbrand, L. A., Massey, P., Strom, S. E., & Merrill, K. M. 1993, AJ, 106, 1906
Humphreys, R. M., & McElroy, D. B. 1984, ApJ, 284, 565
Landolt, A. U. 1983, AJ, 88, 439
Luhman, K. L., Rieke, G. H., Lada, C. J., & Lada, E. A. 1998, ApJ, 508, 347
Massey, P., & Johnson, J. 1993, AJ, 105, 980
Massey, P., Lang, C. C., DeGioia-Eastwood, K., & Garmany, C. D. 1995, ApJ, 438, 188
Marraco, H. G., Vega, E. I., & Vrba, F. J. 1993, AJ, 105, 258
Megeath, S. T., Cox, P., Bronfman, L., & Roelfsema, P. R. 1996, A&A, 305, 296
Morrell, N., Garcia, B., & Levato, H. 1988, PASP, 100, 1431
Norman, C., & Silk, J. 1980, ApJ, 238, 158
Palla, F., & Stahler, S. W. 1990, ApJ, 360, L47
Palla, F., & Stahler, S. W. 1992, ApJ, 392, 667
Palla, F., & Stahler, S. W. 1993, ApJ, 418, 414
Schaller, G., Schaerer, D., Meynet, G., & Maeder, A. 1992, A&AS, 96, 269
Schechter, P. L., Mateo, M., & Saha, A. 1993, PASP, 105, 1342
Sharpless, S. 1963, in Basic Astronomical Data, ed. K. Aa. Strand (Chicago: Univ. Chicago Press), 232
Stauffer, J. R., Hartmann, L. W., Prosser, C. F., Randich, S., Balachandran, S., Patten, B. M., Simon, T., & Giampapa, M. 1997, ApJ, 479, 776
Tapia, M., Roth, M., Marraco, H., & Ruiz, M. T. 1988, MNRAS, 232, 661
Turner, D. G., & Moffat, A. F. J. 1980, MNRAS, 192, 283
Vazquez, R. A., Baume, G., Feinstein, A., & Prado, P. 1996, A&AS, 116, 75
Walborn, N. R. 1971, ApJ, 167, L31
Walborn, N. R. 1973, ApJ, 179, 517
Warner, J. W., Strom, S. E., & Strom, K. M. 1977, ApJ, 213, 427
Westphal, J. A., & Neugebauer, G. 1969, ApJ, 156, L45